Zheng et al. BMC Plant Biology (2019) 19:255
https://doi.org/10.1186/s12870-019-1788-9

BMC Plant Biology

RESEARCH ARTICLE Open Access

Elevated CO_2 concentration induces photosynthetic down-regulation with changes in leaf structure, non-structural carbohydrates and nitrogen content of soybean

Yunpu Zheng[1], Fei Li[1], Lihua Hao[1*], Jingjin Yu[2], Lili Guo[1], Haoran Zhou[3], Chao Ma[1], Xixi Zhang[1] and Ming Xu[4,5*]

Abstract

Background: Understanding the mechanisms of crops in response to elevated CO_2 concentrations is pivotal to estimating the impacts of climate change on the global agricultural production. Based on earlier results of the "doubling-CO_2 concentration" experiments, many current climate models may overestimate the CO_2 fertilization effect on crops, and meanwhile, underestimate the potential impacts of future climate change on global agriculture ecosystem when the atmospheric CO_2 concentration goes beyond the optimal levels for crop growth.

Results: This study examined the photosynthetic response of soybean (*Glycine max* (L.) Merr.) to elevated CO_2 concentration associated with changes in leaf structure, non-structural carbohydrates and nitrogen content with environmental growth chambers where the CO_2 concentration was controlled at 400, 600, 800, 1000, 1200, 1400, 1600 ppm. We found CO_2-induced down-regulation of leaf photosynthesis as evidenced by the consistently declined leaf net photosynthetic rate (A_n) with elevated CO_2 concentrations. This down-regulation of leaf photosynthesis was evident in biochemical and photochemical processes since the maximum carboxylation rate (V_{cmax}) and the maximum electron transport rate (J_{max}) were dramatically decreased at higher CO_2 concentrations exceeding their optimal values of about 600 ppm and 400 ppm, respectively. Moreover, the down-regulation of leaf photosynthesis at high CO_2 concentration was partially attributed to the reduced stomatal conductance (G_s) as demonstrated by the declines in stomatal density and stomatal area as well as the changes in the spatial distribution pattern of stomata. In addition, the smaller total mesophyll size (palisade and spongy tissues) and the lower nitrogen availability may also contribute to the down-regulation of leaf photosynthesis when soybean subjected to high CO_2 concentration environment.

Conclusions: Down-regulation of leaf photosynthesis associated with the changes in stomatal traits, mesophyll tissue size, non-structural carbohydrates, and nitrogen availability of soybean in response to future high atmospheric CO_2 concentration and climate change.

Keywords: CO_2 enhancement, Down regulation, Non-structural carbohydrates, N availability, Stomatal traits, Soybean crops

* Correspondence: haolihua_000@sina.com; mingxu@henu.edu.cn
[1]School of Water Conservancy and Hydropower, Hebei University of Engineering, Handan 056038, China
[4]Key Laboratory of Geospatial Technology for the Middle and Lower Yellow River Regions, College of Environment and Planning, Henan University, Kaifeng 475004, China
Full list of author information is available at the end of the article

Background

It is well known that human activities have dramatically increased atmospheric concentrations of greenhouse gases [1, 2], particularly the elevated atmospheric carbon dioxide concentration due to fossil fuel combustion and land use change following the nineteenth century industrial revolution [3–5]. The most recently released report by the Inter-governmental Panel on Climate Change (IPCC) [6] showed that global atmospheric CO_2 concentration has been dramatically increased from 280 ppm (the pre-industrial level) to over 400 ppm (the present level) with the growth rate of CO_2 concentration by ~1.0 ppm per year [6], and may even be over 1000 ppm at the end of this century [7]. The elevated atmospheric CO_2 concentration may lead to drastic impacts on the structure and function of natural and managed ecosystems [8–12].

Plant responses to elevated CO_2 concentration are fundamentally mediated by leaf photosynthesis, which is closely associated with the changes in leaf structure, chemical composition and carbon balance depending on plant species and/or functional types [13–15]. Many previous studies have shown that elevated CO_2 generally stimulated the net photosynthetic rate (A_n) of plants, namely "CO_2 fertilization effect", especially for the C_3 species, because the ribulose-1, 5-bisphophate carboxylase/oxygenase (Rubisco) of C_3 plants is not CO_2-saturated at the current atmospheric CO_2 concentration [14, 16–21]. Meanwhile, the enhanced A_n may also be resulted from the reduced photorespiration and dark respiration and enhanced carboxylation efficiency under high CO_2 concentrations [22–25]. However, other studies reported that the A_n was not marginally enhanced and even declined when plants exposed to long-term elevated CO_2 concentrations [26–28]. For example, Kanemoto [29] found that leaf photosynthesis of soybean plants was substantially decreased with elevating CO_2 concentration from about 400 ppm to 1000 ppm for 27 days of treatment. This down-regulation of A_n may be attributed to the lower Rubisco concentration and activity [30–34] or/and the source-sink imbalance due to leaf carbohydrates accumulation under elevated CO_2 concentration [29, 35–38]. In addition, the down-regulation of A_n at high CO_2 concentration may also be caused by the decline of stomatal conductance [4, 39–46]. Xu [47] found that the decline in biomass of winter wheat at high CO_2 concentration might be attributed to the decrease of G_s mainly due to the reduction in stomatal length and stomatal density.

In addition to physiological traits, leaf structural and biochemical characteristics may also play a pivotal role in plant response to high CO_2 concentration [48–50]. Elevated CO_2 concentration usually generates greater leaf thickness and total mesophyll size, which closely correlated to leaf photosynthetic rate [51–54]. Previous studies have shown that elevated CO_2 concentration increased the leaf thickness and mesophyll cross-section area, which was mainly attributable to greater cell expansion rather than enhanced cell division due to the increase of carbohydrate substrate availability [55–57]. The thicker mesophyll tissue and larger cell volume may provide more space for accommodating chloroplasts and more intercellular surface area for leaf gas exchange [42, 58–60]. Meanwhile, elevated CO_2 concentration may also change leaf biochemical compositions including the non-structural carbohydrates and nitrogen concentration (N), which play an important role in controlling over the responses of plants and/or ecosystems to rising atmospheric CO_2 levels [17, 61, 62]. Understanding the mechanisms of leaf structure and biochemistry in response to high CO_2 concentration is critical for assessing the changes in leaf functional traits and thus ecosystem functioning under future global change.

Several previous studies have documented that different plants features with different optimal CO_2 concentrations for plant growth [47, 63] and thus plants with high optimal CO_2 concentrations will suffer less from climate change and meanwhile benefit the most from the CO_2 fertilization effect due to high nitrogen and water use efficiency [24]. Exploring the mechanisms of CO_2 fertilization effect on crops is critical to estimating global agriculture yield under climatic change [64]. Numerous studies have investigated CO_2 fertilization effect primarily focusing on the impact of twofold current [CO_2] on plants with doubling CO_2 concentration experiment [64–66], which normally increased CO_2 concentration from 300 to 400 ppm to the projected atmospheric CO_2 concentration of 600–800 ppm at the end of the next century [6, 67]. However, the atmosphere CO_2 concentration has covered a much wider range throughout geological time scales with an estimated value of 6000 ppm during the Paleozoic Era about 500 million years ago [24]. To our knowledge, few studies have examined the responsible mechanism of A_n associated with changes in leaf structure, non-structural carbohydrates and nitrogen content of soybean (*Glycine max* (L.) Merr.), the fourth important crop species in the world under higher CO_2 concentrations beyond the twofold current CO_2 concentration of 800 ppm. Therefore, we conducted this experiment with environmental growth chambers controlling multiple high CO_2 levels from 400 ppm to 1600 ppm to test the following hypotheses:

(1) Leaf photosynthesis is down-regulated at higher CO_2 concentrations beyond the optimal atmospheric CO_2 concentration for the growth of soybean (HY1).
(2) This down-regulation of leaf photosynthesis may attribute to the declines in biochemical and photochemical efficiency such as the maximum

carboxylation rate (V_{cmax}) and the maximum electron transport rate (J_{max}) (HY2).

(3) The CO_2-induced stomatal closure and irregular distribution pattern of stomata on soybean leaves will partially explain the down-regulation of leaf photosynthesis under high CO_2 concentrations (HY3).

(4) Changes in leaf mesophyll anatomy and chemical composition may also play essential roles in the down-regulation processes of leaf photosynthesis when soybean subjected to elevated atmospheric CO_2 concentrations (HY4).

Results

CO_2 effects on leaf photosynthesis, stomatal conductance, water use efficiency, and dark respiration

We found a negative quadratic relationship between leaf photosynthesis and CO_2 concentration ($R^2 = 0.83$) with the minimum leaf photosynthesis occurred at the CO_2 concentration of 1200 ppm (Fig. 1a). Similar with the leaf photosynthesis, elevated CO_2 concentrations resulted in non-linear decrease in stomatal conductance, which followed a quadratic relationship ($R^2 = 0.91$) with the minimum value occurring around 1200 ppm (Fig. 1b). Meanwhile, a quadratic equation can also be used to describe the relationship ($R^2 = 0.51$) between the leaf-level water use efficiency (*WUE*) and the CO_2 concentration (Fig. 1c). However, the leaf dark respiration rate demonstrated a bell-shaped curve ($R^2 = 0.60$) peaking at 900 ppm in relation to CO_2 concentration (Fig. 1d).

CO_2 effects on V_{cmax}, J_{max}, and the V_{cmax} /J_{max} ratio

Both the maximum carboxylation rate (V_{cmax}) and the V_{cmax}/J_{max} ratio in response to increasing CO_2 concentration featured bell-shaped curves, peaking at 592.5 ppm (Fig. 2a) and 666.7 ppm (Fig. 2c), respectively. However, the increase in CO_2 concentration led to a non-linear decline in the maximum electron transport rate (J_{max}) with the maximum value occurring around 390 ppm (Fig. 2b). These relationships of V_{cmax}, J_{max}, and V_{cmax}/J_{max} ratio in relation to CO_2 concentration could be described by quadratic equations with R^2 values of 0.85. 0.76, and 0.74, respectively (Fig. 2).

CO_2 effects on morphological traits and spatial distribution pattern of stomata

We found that the stomatal area was substantially enhanced by 37% on the adaxial surfaces enhancing CO_2 concentration from 400 to 1200 ppm ($p = 0.03$), although stomatal length, width, perimeter and shape index were barely affected by elevated CO_2 concentration ($p > 0.05$; Table 1; Fig. 3). Our results also showed that elevated CO_2 concentration significantly decreased stomatal area index on both the adaxial and abaxial leaf surfaces

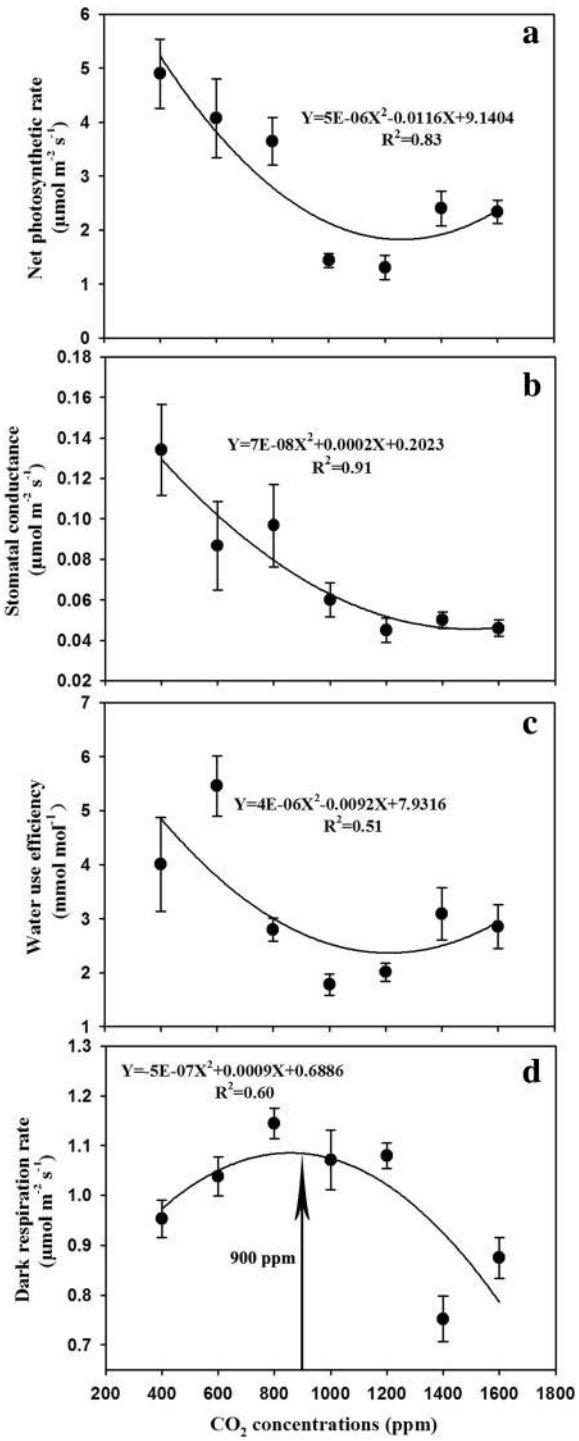

Fig. 1 Effects of elevated CO_2 concentrations on (**a**) leaf net photosynthesis rate (A_n), (**b**) stomatal conductance (G_s), (**c**) intercellular CO_2 concentration (C_i), and (**d**) dark respiration rate (R_d). Parameters are measured at ambient or elevated CO_2 of their growing condition for each treatment and values given are mean ± standard deviation for n = 5 leaves. The arrow indicates the optimal CO_2 concentration for leaf R_d of soybean plants

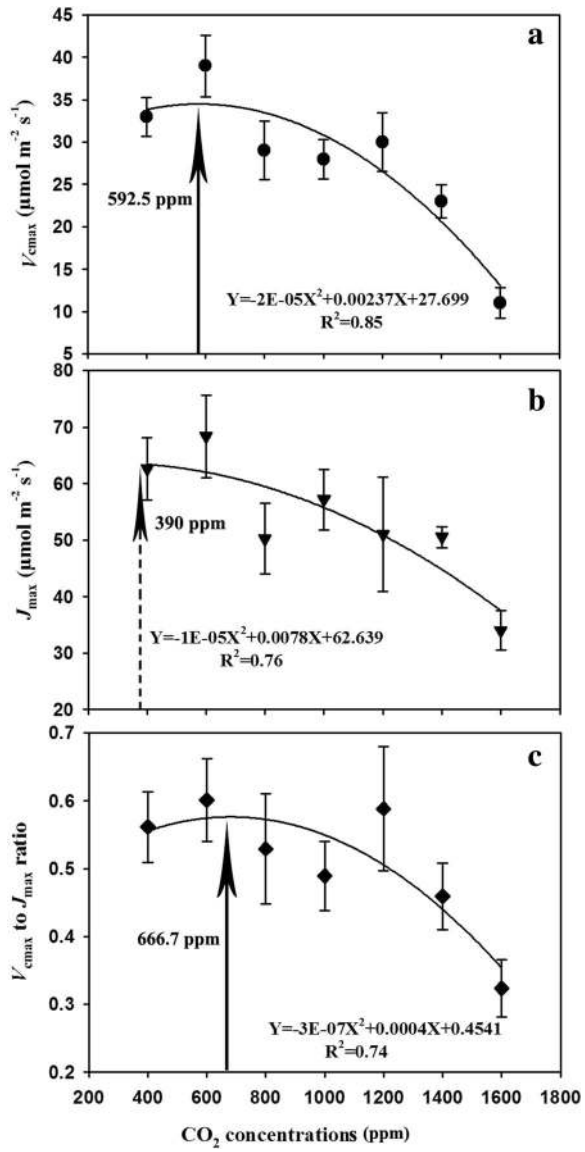

Fig. 2 Effects of elevated CO_2 concentrations on the V_{cmax} (a), J_{max} (b) and V_{cmax}/J_{max} ratio of soybean plants

except for increasing CO_2 concentration from 400 to 600 ppm, where the stomatal area index on the abaxial side was marginally increased by 15% and reached its maximum value at 600 ppm (Table 1; Fig. 3). By contrast, the stomatal area index on the adaxial surface was significantly decreased by about 60% with the increase of CO_2 concentration from 400 to 600 ppm and reached its minimum value at 600 ppm (Table 1; Fig. 3). Moreover, our results also showed that the stomatal density on the adaxial side was decreased by about 57% ($p = 0.01$), 61% ($p = 0.013$), 38% ($p = 0.025$), 32% ($p = 0.026$) and 48% ($p = 0.003$) with increasing CO_2 concentration to 600, 800, 1200, 1400, and 1600 ppm, respectively (Table 1; Fig. 3). However, elevating CO_2 concentration from 400 to 600 ppm made the stomatal density on the abaxial sides increased 21% (Table 1; Fig. 3). In addition, we also found the interactive effect of leaf surface and CO_2 concentration on the stomatal density ($p = 0.009$) and stomatal area ($p = 0.006$; Table 2).

Elevated CO_2 concentration not only changed the morphological traits of individual stoma but also affected stomatal distribution on soybean leaves. We found that the spatial distribution pattern of stomata was highly scale-dependent with regular patterns at small scales of about 70–170 μm (below the lower 95% envelope) and random patterns at larger scales up to 200 μm (between the upper and lower 95% envelope) on both leaf surfaces (Fig. 4). Increasing CO_2 concentration from 400 to 600 ppm caused the stomatal distribution to become more regular at small scales on the adaxial surface as evidenced by the decrease of Lhat (d) value from − 1.69 to − 12.00. However, the stomata on the abaxial surfaces tend to be less regular than those on the adaxial surface because the abaxial surface had higher Lhat (d) values at the same scale (Fig. 4). In addition, elevated CO_2 concentration increased the scale range of regular distribution from 50 μm to 180 μm on the adaxial surface (Fig. 4a), while the scale range of regular distribution on the abaxial surface was decreased from 160 μm to 100 μm (Fig. 4b). In general, this enhanced CO_2 concentration effect on the spatial distribution pattern of stomata was greater on the adaxial surface than the abaxial surface of soybean leaves.

CO_2 effects on leaf anatomic characteristics

Elevated CO_2 concentration significantly increased cell length, whereas decreased cell width of palisade mesophyll (PM) ($p < 0.05$; Table 3; Fig. 5). Elevating CO_2 concentration from 400 ppm to 1000 ppm made the cell length of palisade layer increased from about 36 μm to 42 μm (Table 3). Relative to ambient CO_2 concentration, the cell size of palisade layer was also significantly affected by elevated CO_2 concentration (Fig. 5). Enhancing CO_2 concentration from 400 ppm to 1000 ppm resulted in increases of cell area and cell perimeter by about 10 and 20%, mainly due to the larger cell length of PM. Elevated CO_2 concentration from 400 ppm to 1000 ppm caused a decrease in the cell width of palisade by 23% (Table 3). Moreover, the cell length of spongy mesophyll (SM) was substantially enhanced by 32%, and thus the cell area was increased by 25% with elevating CO_2 concentration of 1000 ppm. In addition, elevated CO_2 concentration significantly affected both the thickness (LT) and the palisade/spongy ratio of soybean leaves ($p < 0.05$; Fig. 5).

CO_2 effects on tissue carbon and nitrogen

Elevated CO_2 concentration dramatically affected tissue carbon (C) and nitrogen (N) as well as C/N of soybean plants (Table 4). Specifically, increasing CO_2 concentration

Table 1 Effects of CO_2 concentrations on the stomatal density and morphological traits of individual stoma

Stomatal parameters	CO_2 concentration (ppm)							
	400	600	800	1000	1200	1400	1600	*p* value
Adaxial surface								
Stomatal length (μm)	9.4 ± 1.3 (a)	9. 7 ± 1.6 (a)	9.6 ± 0.6 (a)	9.6 ± 0.8 (a)	9.0 ± 2.0 (a)	9.50 ± 0.5 (a)	9.8 ± 1.6 (a)	$p > 0.05$
Stomatal width (μm)	2.2 ± 0.9 (a)	1.8 ± 0.4 (a)	2.6 ± 0.5 (a)	1.7 ± 0.2 (a)	2.7 ± 0.5 (a)	2.4 ± 0.5 (a)	2.5 ± 0.7 (a)	$p > 0.05$
Stomatal area (μm^2)	92.6 ± 16.2 (b)	88.7 ± 9.6 (b)	105.4 ± 5.2 (ab)	83.3 ± 9.0 (b)	126.4 ± 24.1 (a)	100.3 ± 17.2 (b)	103.9 ± 11.0 (ab)	$p = 0.03$
Stomatal perimeter (μm)	40.7 ± 0.5 (ab)	45.0 ± 1.0 (ab)	41.0 ± 0.1 (ab)	37.9 ± 0.2 (b)	46.2 ± 0.4 (a)	40.5 ± 0.3 (ab)	41.2 ± 0.27 (ab)	$p > 0.05$
Stomatal density (No./mm^2)	16.8 ± 8.9 (a)	7.3 ± 4.9 (c)	6.6 ± 4.7 (bc)	17.8 ± 5.3 (a)	10.4 ± 6.4 (bc)	11.4 ± 6.3 (b)	8.7 ± 3.5 (b)	$p = 0.04$
Stomatal shape index (%)	24.0 ± 1.3 (a)	20.4 ± 4.7 (b)	25.0 ± 0.2 (a)	24.1 ± 0.2 (a)	24.3 ± 2.4 (a)	24.6 ± 0.6 (a)	24.7 ± 0.7 (a)	$p > 0.05$
Stomatal area index (%)	9.4 ± 1.7 (a)	3.9 ± 0.4 (d)	4.2 ± 0.3 (d)	9.0 ± 1.0 (a)	7.9 ± 1.5 (ab	6.9 ± 1.2 (bc)	5.4 ± 0.6 (cd)	$p < 0.001$
Abaxial surface								
Stomatal length (μm)	9.6 ± 1.7 (ab)	9.8 ± 0.6 (ab)	9.5 ± 0.8 (ab)	10.2 ± 0.7 (a)	8.9 ± 0.6 (b)	9.4 ± 0.2 (ab)	9.2 ± 0.1 (ab)	$p > 0.05$
Stomatal width (μm)	3.1 ± 0.9 (a)	3.1 ± 0.3 (a)	3.2 ± 0.3 (a)	2.9 ± 0.4 (a)	3.0 ± 0.4 (a)	3.1 ± 0.2 (a)	2.8 ± 0.1 (a)	$p > 0.05$
Stomatal area (μm^2)	133.1 ± 0.5 (a)	123.9 ± 16.5 (ab)	108.9 ± 13.8 (bc)	102.3 ± 6.1 (c)	109.3 ± 7.5 (bc)	113.9 ± 9.2 (abc)	110.1 ± 17.8 (bc)	$p > 0.05$
Stomatal perimeter (μm)	42.8 ± 5.5 (a)	44.6 ± 2.8 (a)	41.1 ± 3.1 (a)	40.7 ± 1.4 (a)	40.7 ± 2.0 (a)	42.6 ± 1.7 (a)	41.8 ± 3.3 (a)	$p > 0.05$
Stomatal density (No./mm^2)	101.3 ± 20.1 (abc)	128.3 ± 18 (a)	95.7 ± 10.8 (bc)	92 ± 17.0 (c)	104.8 ± 9.7 (abc)	84.2 ± 9.2 (c)	111.4 ± 17.8 (ab)	$p > 0.05$
Stomatal shape index (%)	25.3 ± 0.1 (a)	24.9 ± 0.1 (a)	25.2 ± 0.4 (a)	24.9 ± 0.1 (a)	25.1 ± 0.5 (a)	25.0 ± 0.4 (a)	25.1 ± 0. (a)	$p > 0.05$
Stomatal area index (%)	81.9 ± 0.3 (b)	96.3 ± 12.8 (a)	63.2 ± 8.0 (cd)	57.1 ± 3.4 (d)	69.5 ± 4.8 (bcd))	58.2 ± 4.72 (d)	74.8 ± 12.1 (bc)	$p < 0.001$
Adaxial/abaxial ratio	0.23 ± 0.023 (ab)	0.12 ± 0.022 (c)	0.13 ± 0.042 (c)	0.26 ± 0.002(a)	0.21 ± 0.018 (b)	0.20 ± 0.013 (b)	0.09 ± 0.024 (c)	$p < 0.001$

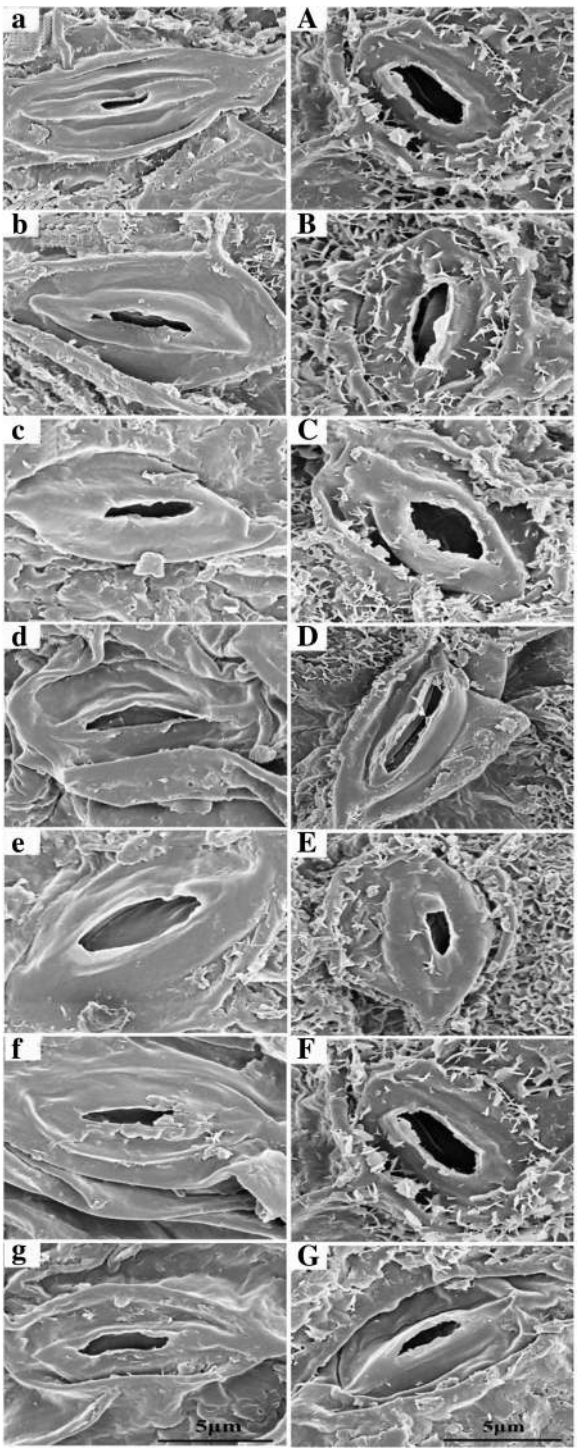

Fig. 3 Changes in the morphological traits of stomata on the adaxial leaf surface (**a**-**g**) and abaxial leaf surface (**A**-**G**) of soybean leaves grown at CO_2 concentrations of 400, 600, 800, 1000, 1200, 1400 and 1600 ppm observed with scanning electron microscopy. Bars = 5 μm

Table 2 Effects of CO_2 concentrations on the stomatal parameters at different leaf surfaces of soybean

Parameters	SD (No. mm^{-2})	SL (mm)	SW (mm)	SA (mm^2)	SP (mm)	SAI (%)	SSI (%)
CO_2	0.149	0.531	0.352	0.102	0.910	0.194	0.130
Leaf surface	< 0.001	< 0.001	< 0.001	< 0.001	0.805	0.933	0.002
CO_2 × Leaf surface	0.009	0.158	0.350	0.006	0.269	0.323	0.290

Note: *SD* is stomatal density, *SL* is stomatal length, *SW* is stomatal width, *SA* is stomatal area, *SP* is stomatal perimeter, *SAI* is stomatal area index, and *SSI* is stomatal shape index

from 400 ppm to 1000 ppm substantially decreased C concentrations of leaf and stem ($p < 0.001$), whereas the root C content was significantly increased by 5% from 354.8 mg g^{-1} to 371.2 mg g^{-1} with further increasing CO_2 concentration from 1000 ppm to 1600 ppm ($p < 0.001$). Moreover, elevated CO_2 concentration enhanced the N content of stem and root (Table 4), while the leaf N was significantly decreased from 32.0 mg g^{-1} to 30.8 mg g^{-1} with increasing CO_2 concentration from 400 ppm to 1200 ppm ($p < 0.001$; Table 4). Elevated CO_2 concentration decreased the tissue C/N ratio due mainly to the increased N and decreased C in stems and roots ($p < 0.001$; Table 4). In addition, enhancing CO_2 concentration from 400 ppm to 800 ppm slightly increased the leaf, stem, and total TNC by 12.8, 4.9, and 5.9%, whereas the TNC in leaves and stems were dramatically reduced with further increasing CO_2 concentration from 800 ppm to 1600 ppm (Table 5).

Relationships among photosynthesis, leaf structure, non-structural carbohydrates, and nitrogen content

We estimated the relationships between photosynthesis and stomatal conductance as well as photosynthesis and stomatal area and found that leaf photosynthesis was increased linearly by the enhancement of stomatal conductance and stomatal area on the adaxial surface with R^2 values of 0.81 ($p = 0.01$) and 0.67 ($p = 0.02$), respectively (Fig. 6a-b). In contrast to the stomatal area on the adaxial surface, we found no linear relationship between leaf photosynthesis and stomatal area on the abaxial surface of soybean plants ($R^2 = 0.07$, $p = 0.60$; Fig. 6c). Moreover, we also found that leaf photosynthesis was linearly increased by the cell enlargement of spongy and palisade tissues with R^2 values of 0.74 ($p = 0.01$) for spongy cell area and 0.72 ($p = 0.02$) for palisade cell area, respectively (Fig. 7). In addition to leaf structure, we also evaluated the relationship among leaf photosynthesis, carbohydrates and nitrogen content. We found a positive but not significative relationship between leaf photosynthesis and non-structural carbohydrate content following a linear equation ($R^2 = 0.44$, $p = 0.11$; Fig. 8).

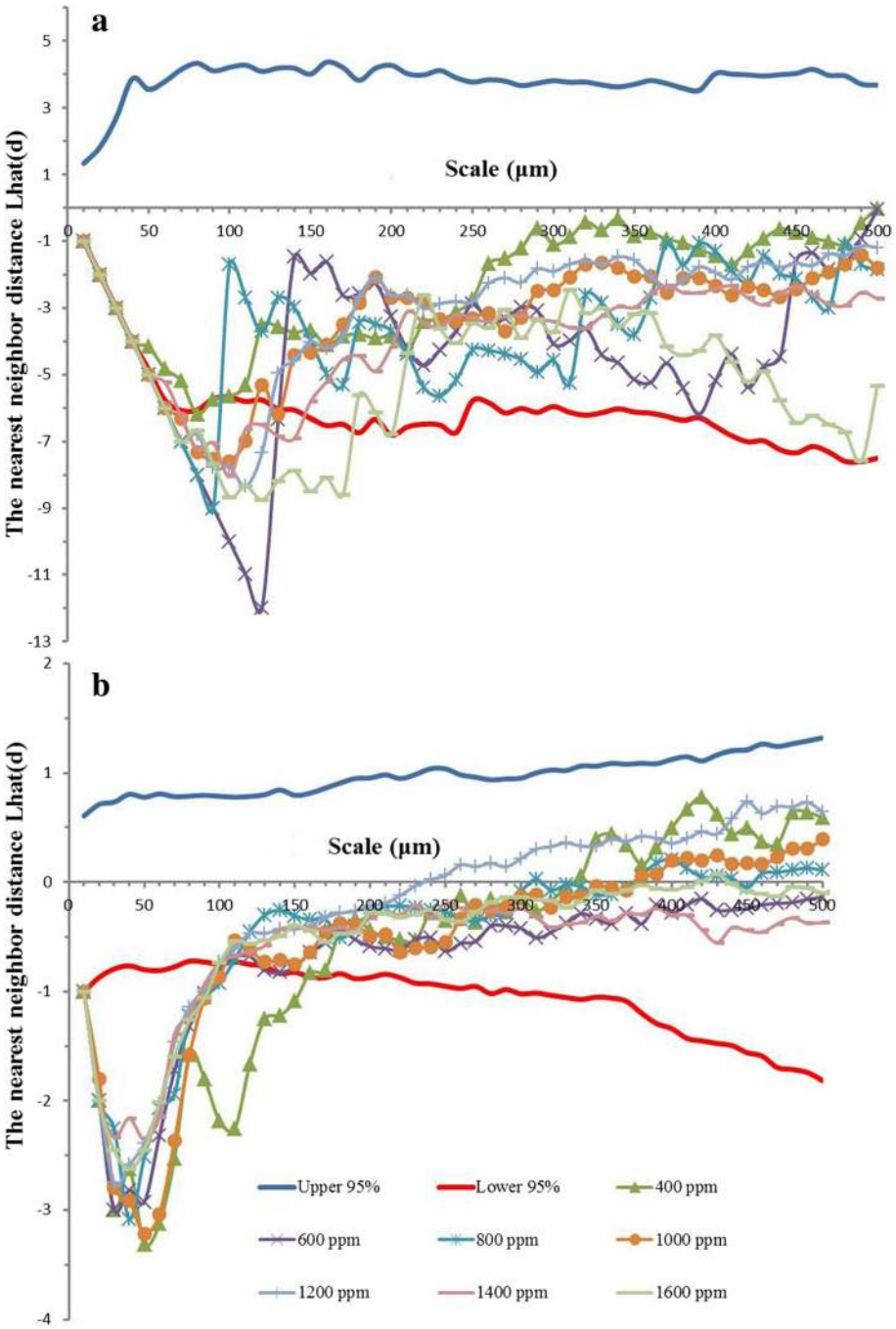

Fig. 4 The spatial distribution pattern of stomata on the adaxial surface (**a**) and abaxial surface (**b**) of soybean leaves under elevated CO_2 concentrations. The upper and lower 95% boundaries were obtained by Monte Carlo simulation of 100 replicates

Discussion

Down-regulation of leaf photosynthesis under elevated atmospheric CO_2 concentrations

It is demonstrated that elevated CO_2 concentration generally stimulates plant growth and enhanced crop yield through the CO_2 fertilization effect [17, 18], whereby augmented atmosphere CO_2 concentration can directly boost carboxylation in the Calvin-Benson-Bassham cycle and competitively inhibit dark respiration and photorespiration [13, 16]. By contrast, several studies claim that some plants may develop an adverse response through a process known as "down-regulation" of photosynthesis when plants exposed to higher CO_2 concentration beyond certain thresholds [4, 26, 28]. We also found a negative

Table 3 Effects of elevated CO_2 concentrations on the morphological and anatomical traits of soybean

Parameters	CO_2 concentrations (ppm)							*p* value
	400	600	800	1000	1200	1400	1600	
Palisade layer								
Cell length (μm)	35.69 ± 3.04 (c)	39.14 ± 3.43 (ab)	38.59 ± 34.46 (b)	42.03 ± 5.23 (a)	33.38 ± 6.24 (d)	29.76 ± 4.47 (e)	41.15 ± 7.35 (a)	$p < 0.001$
Cell width (μm)	9.35 ± 1.76 (b)	8.93 ± 1.78 (b)	7.90 ± 31.22 (de)	9.00 ± 1.50 (bc)	7.25 ± 1.29 (e)	10.40 ± 1.18 (a)	8.13 ± 2.00 (cd)	$p < 0.001$
Cell area (μm^2)	303.3 ± 39.6 (b)	348.7 ± 39.4 (a)	275.0 ± 76.2 (c)	328.0 ± 80.9 (ab)	213.1 ± 46.3 (d)	232.1 ± 60.5 (d)	303.5 ± 88.9 (bc)	$p < 0.001$
Cell perimeter (μm)	83.0 ± 6.4 (c)	95.1 ± 12.6 (b)	80.6 ± 9.9 (c)	99.3 ± 12.7 (ab)	71.4 ± 9.4 (d)	67.6 ± 10.2 (d)	100.9 ± 19.3 (a)	$p < 0.001$
Spongy layer								
Cell length (μm)	20.72 ± 2.43 (cd)	24.85 ± 4.00 (ab)	22.61 ± 5.45 (bc)	27.36 ± 7.75 (a)	19.87 ± 3.11 (d)	20.15 ± 2.87 (d)	20.07 ± 5.11 (d)	$p = 0.009$
Cell width (μm)	11.91 ± 3.13 (b)	12.04 ± 3.75 (a)	9.39 ± 5.44 (d)	10.54 ± 3.71 (ac)	8.28 ± 2.14 (e)	12.68 ± 2.15 (ad)	8.46 ± 2.40 (bef)	$p < 0.001$
Cell area (μm^2)	207.8 ± 57.6 (b)	265.3 ± 88.4 (a)	192.0 ± 64.5 (b)	258.9 ± 24.5 (a)	150.0 ± 43.8 (c)	215.6 ± 53.0 (b)	177.2 ± 67.7 (b)	$p = 0.010$
Cell perimeter (μm)	86.2 ± 13.2 (bc)	76.88 ± 13.8 (a)	60.6 ± 13.3 (c)	71.4 ± 21.7 (ab)	55.5 ± 12.0 (d)	55.6 ± 13.7 (d)	63.1 ± 15.5 (bcd)	$p = 0.020$
Palisade/Spongy ratio	1.88 ± 0.68 (b)	2.52 ± 0.23 (a)	2.59 ± 0.64 (ab)	2.77 ± 0.54 (a)	2.13 ± 0.60 (abc)	1.90 ± 0.49 (bc)	1.75 ± 0.25 (c)	$p < 0.031$
Leaf thickness (μm)	103.5 ± 11.0 (c)	126.9 ± 9.9 (a)	121.5 ± 9.9 (b)	125.4 ± 12.7 (b)	108.7 ± 14.1 (c)	108.0 ± 12.2 (c)	106.9 ± 11.1 (c)	$p = 0.001$

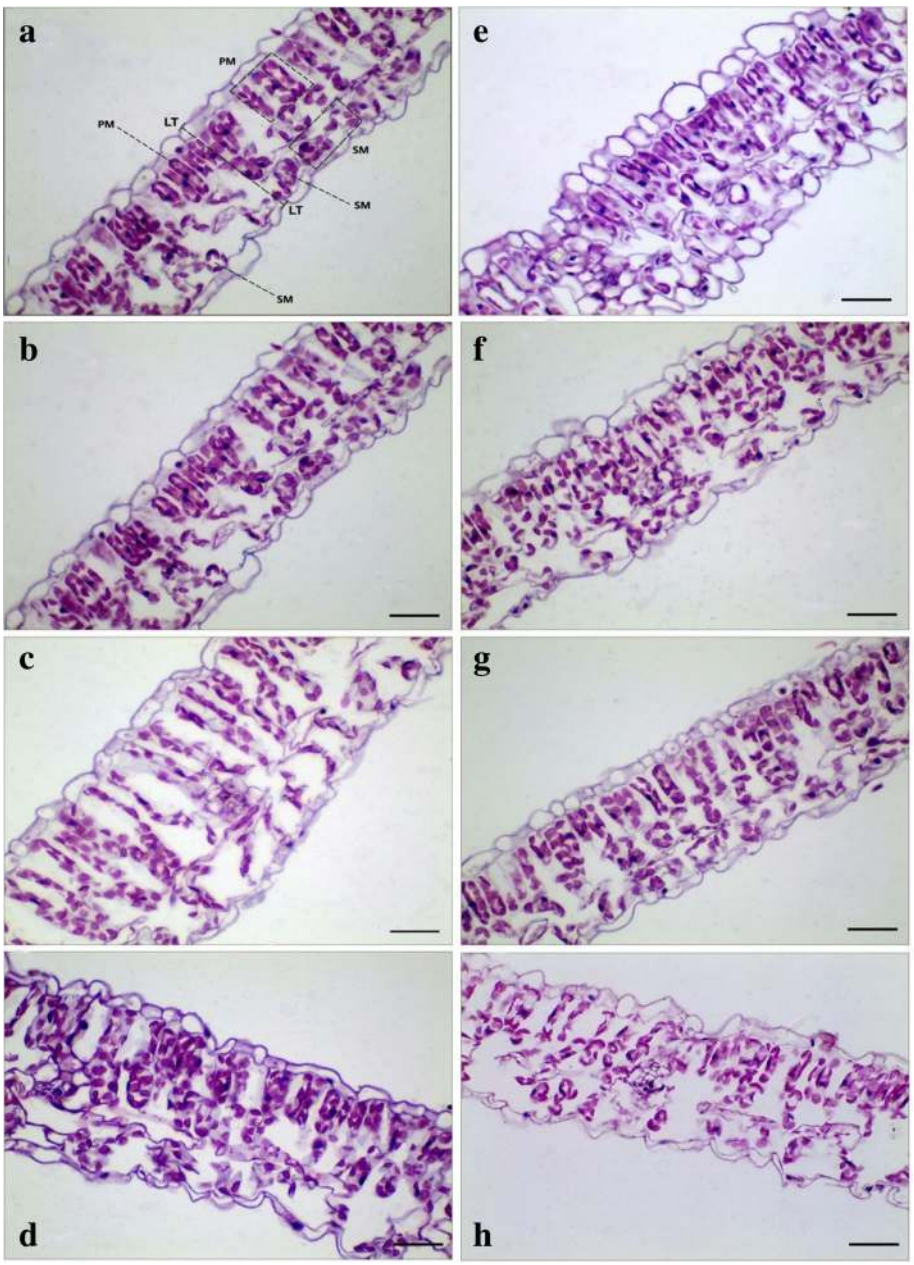

Fig. 5 Light micrographs of cross-section through leaves of soybean. Note that cross-section micrographs show leaf thickness (LT), palisade mesophyll (PM), and spongy mesophyll (SM) of soybean leaves grown at ambient (**a**-**b**) and elevated CO_2 concentrations (c-h). Bar = 50 μm

quadratic relationship between leaf photosynthesis and CO_2 concentration ($R^2 = 0.83$; Fig. 1), indicating down-regulation of leaf photosynthesis did occur when soybean plants subjected to enhanced CO_2 concentrations. This down-regulation of leaf photosynthesis may be caused by various limiting factors such as lower Rubisco concentration and activity [29, 30, 32, 34] reduced stomatal conductance [15, 68, 69], and excessive carbohydrates accumulation in leaves [29, 36–38].

Further analysis showed that leaf biochemical and photochemical efficiency might play a pivotal role in the down-regulation of leaf photosynthesis in the current study. Our results showed that the maximum carboxylation rate of Rubisco (V_{cmax}) and the maximum capacity of electron transport RuBP regeneration (J_{max}) were dramatically decreased by elevated CO_2 concentrations, suggesting that enhanced CO_2 concentrations may affect both the light and dark reactions of photosynthesis.

Table 4 Effects of elevated CO_2 concentrations on carbon and nitrogen contents of soybean

Element (mg g^{-1} DW)		CO_2 concentrations (ppm)							*p* value
		400	600	800	1000	1200	1400	1600	
Leaf	C	403.6 ± 0.33(a)	386.14 ± 0.23(d)	390.54 ± 0.24 (d)	373.66 ± 12.73 (c)	393.30 ± 0.70 (bd)	392.07 ± 0.50 (bd)	395.71 ± 0.37(ab)	$p < 0.001$
	N	32.04 ± 0.12 (bc)	30.56 ± 0.22 (d)	33.56 ± 0.16 (a)	31.61 ± 1.00 (c)	34.04 ± 0.12 (a)	32.61 ± 0.07 (b)	30.83 ± 0.2 (d)	$p < 0.001$
	C/N	12.60 ± 0.05 (b)	12.64 ± 0.10 (b)	11.64 ± 0.06 (e)	11.82 ± 0.03 (d)	11.55 ± 0.03 (e)	12.02 ± 0.04 (c)	12.84 ± 0.08 (a)	$p < 0.001$
Stem	C	375.71 ± 0.66 (a)	358.33 ± 0.47 (b)	348.84 ± 0.17(d)	347.86 ± 0.20 (e)	335.51 ± 0.05 (g)	339.93 ± 1.01(f)	359.40 ± 0.30 (c)	$p < 0.001$
	N	26.47 ± 0.14(g)	32.58 ± 0.19 (f)	43.24 ± 0.25 (b)	45.85 ± 0.41 (a)	37.51 ± 0.10 (d)	42.24 ± 0.12 (c)	36.94 ± 0.20 (e)	$p < 0.001$
	C/N	14.19 ± 0.09 (a)	10.10 ± 0.06 (b)	8.07 ± 0.05 (e)	7.59 ± 0.07 (f)	8.95 ± 0.023.6 (d)	8.05 ± 0.04 (e)	9.73 ± 0.06 (c)	$p < 0.001$
Root	C	352.38 ± 0.13 (cd)	347.81 ± 0.42 (d)	350.68 ± 0.18 (cd)	354.78 ± 0.52 (c)	376.80 ± 0.62 (ab)	378.59 ± 2.97 (a)	371.19 ± 8.64 (b)	$p < 0.001$
	N	26.08 ± 0.29 (c)	34.40 ± 0.19 (b)	38.35 ± 0.09 (a)	37.70 ± 0.10 (a)	36.79 ± 0.25(a)	37.57 ± 0.33 (a)	33.59 ± 3.33 (b)	$p < 0.001$
	C/N	13.51 ± 0.15 (a)	10.11 ± 0.06 (c)	9.14 ± 0.02 (d)	9.41 ± 0.03 (d)	10.24 ± 0.08 (c)	10.07 ± 0.01 (c)	11.10 ± 0.81 (b)	$p < 0.001$

Table 5 Effects of CO_2 concentrations on soluble sugars and starch concentrations of soybean

Non-structural carbohydrate ($mg \cdot g^{-1}$)		CO_2 concentrations (ppm)							*p* value
		400	600	800	1000	1200	1400	1600	
Root	Soluble sugar	58.4 ± 5.0(bc)	96.9 ± 5.7(a)	61.2 ± 5.3(b)	40.1 ± 2.5(d)	63.4 ± 2.0(b)	65.2 ± 3.3(b)	52.1 ± 5.0(c)	$p < 0.001$
	Starch	26.8 ± 3.3(a)	17.2 ± 9.6(b)	25.6 ± 2.3(a)	18.1 ± 2.3(b)	18.4 ± 1.1(b)	20.16 ± 0.96(ab)	13.3 ± 1.5(b)	$p = 0.014$
	TNC	85.3 ± 7.8(b)	114.1 ± 14.8(a)	86.8 ± 6.5(b)	58.1 ± 2.6(c)	81.8 ± 3.0(b)	85.4 ± 3.9(b)	65.4 ± 6.5(c)	$p < 0.001$
Stem	Soluble sugar	51.1 ± 6.4(a)	59.7 ± 4.9(a)	55.8 ± 4.3(a)	64.5 ± 7.4(a)	54.2 ± 3.5(a)	47.2 ± 1.2(a)	53.3 ± 5.1(a)	$p > 0.05$
	Starch	16.2 ± 5.8(bc)	20.2 ± 2.7(ab)	20.2 ± 4.1(ab)	11.7 ± 0.3(c)	23.2 ± 4.1(a)	16.2 ± 0.7(bc)	10.9 ± 3.9(c)	$p < 0.007$
	TNC	67.3 ± 8.3(a)	79.9 ± 7.5(a)	75.9 ± 4.7(a)	76.2 ± 7.6(a)	77.4 ± 3.6(a)	63.4 ± 1.7(a)	64.2 ± 8.7(a)	$p > 0.05$
Leaf	Soluble sugar	65.5 ± 3.9(a)	30.5 ± 5.0(b)	72.6 ± 13.8(a)	59.0 ± 13.3(a)	27.4 ± 1.7(b)	29.7 ± 7.6(b)	22.6 ± 2.7(b)	$p < 0.001$
	Starch	17.9 ± 7.8(c)	26.0 ± 5.3(ab)	14.9 ± 2.0(c)	27.5 ± 4.4(a)	16.9 ± 5.0(c)	15.8 ± 1.7(c)	19.4 ± 1.9(bc)	$p = 0.022$
	TNC	83.4 ± 7.1(a)	56.5 ± 1.5(b)	87.5 ± 15.5(a)	86.5 ± 9.5(a)	44.3 ± 6.4(b)	45.5 ± 5.9(b)	42.0 ± 3.3(b)	$p < 0.001$
Total	Soluble sugar	182 ± 3(abc)	196 ± 27(ab)	212 ± 41 (a)	164 ± 11(bcd)	145 ± 30(cd)	142 ± 10(d)	128 ± 9(d)	$p = 0.004$
	Starch	61.0 ± 11.3(a)	63.4 ± 10.4(a)	60.7 ± 4.4(a)	57.3 ± 6.5(a)	58.5 ± 8.2(a)	52.2 ± 2.4(ab)	43.5 ± 6.4(b)	$p < 0.001$
	TNC	236 ± 7(ab)	250 ± 19(a)	250 ± 16(a)	221 ± 5(bc)	203 ± 27(c)	194 ± 8(cd)	171 ± 15(d)	$p > 0.05$

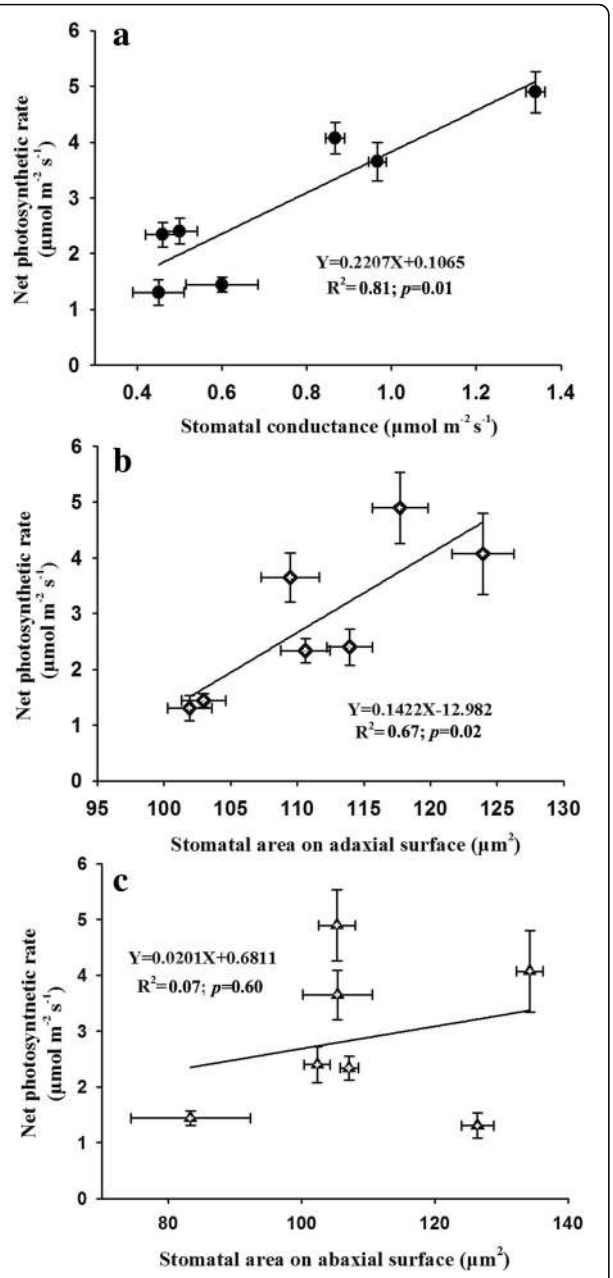

Fig. 6 Effects of elevated CO_2 concentrations on the relationships between net photosynthetic rate and stomatal conductance (**a**) as well as stomatal area (**b** and **c**) of soybean plants

Moreover, our results also suggested that elevated CO_2 may have greater impacts on carboxylation processes than the photochemical processes as indicated by the rapidly decreased V_{cmax}/J_{max} ratio beyond the optimal CO_2 concentration of about 670 ppm (Fig. 2). Therefore, the lower carboxylation and photochemical efficiency as evidenced by the declines of the V_{cmax} and J_{max} values as well as the V_{cmax}/J_{max} ratio at high CO_2 concentrations may explain the negative CO_2 effects on leaf photosynthesis of soybean plants as observed in the current study.

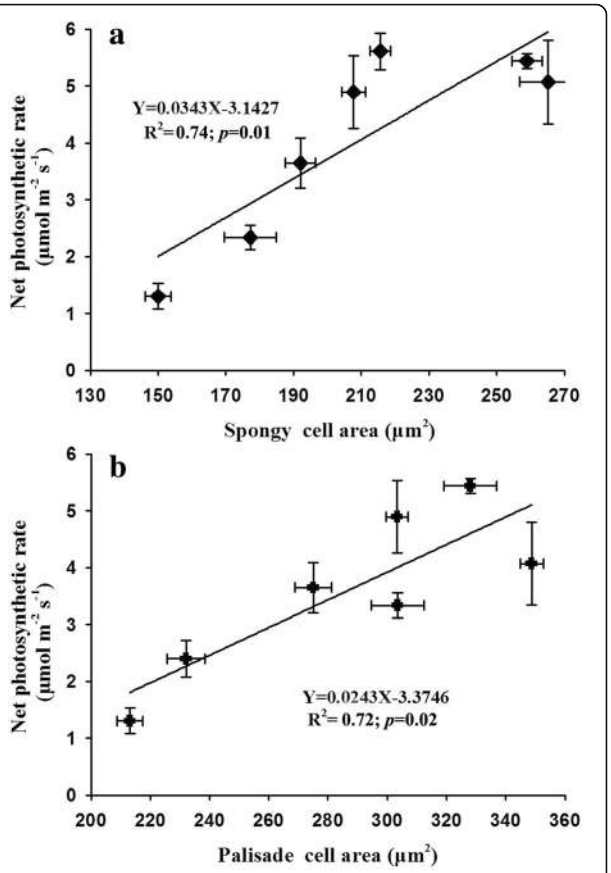

Fig. 7 Effects of elevated CO_2 concentrations on the relationships between net photosynthetic rate and spongy cell area (**a**) or palisade cell area (**b**) of soybean plants

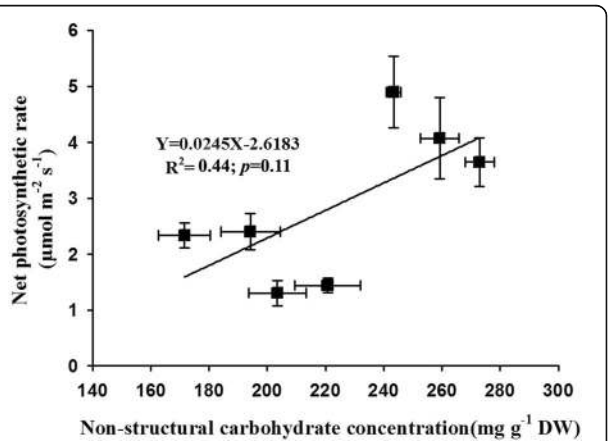

Fig. 8 Effects of elevated CO_2 concentrations on the relationships between net photosynthetic rate and non-structural carbohydrate concentration of soybean plants

Additionally, it is important to note that dark respiration increased with the change of CO_2 from 400 ppm to 900 ppm, which may also contribute to the down-regulation of leaf photosynthesis. However, dark respiration started to decrease when the CO_2 concentration is beyond 900 ppm which offsets the effects of V_{cmax} and J_{max} in the down-regulation of photosynthesis.

Stomatal diffusion processes explain the down-regulation of leaf photosynthesis

In addition to biochemical and photochemical processes, our results also showed that enhancing CO_2 concentrations generally decreased stomatal density on both leaf surface, especially the stomatal density on the adaxial leaf surface was substantially decreased by about 50% with increasing CO_2 concentration from 400 ppm to 1600 ppm (Table 1). This CO_2-induced decrease of stomatal density may explain the down-regulation of leaf photosynthesis because stomatal density partially determines CO_2 diffusion efficiency from atmosphere to mesophyll tissues [52–54] and well correlates with stomatal conductance [47], which is closely associated with leaf photosynthesis [42, 58, 59]. Meanwhile, elevated CO_2 concentrations significantly decreased the total stomatal area per unit leaf area (stomatal area index) on both leaf sides, suggesting the CO_2-induced stomatal closure may also contribute to the decline of leaf photosynthesis through reducing stomatal conductance at high CO_2 concentration. Previous studies have claimed that elevated CO_2 can reduce stomatal openness by changing concentrations of ion and organic solutes and depolarizing the water potential of cell membrane [47, 54, 59].

In the current study, we also found well-correlated relationships among leaf photosynthesis, stomatal conductance, and stomatal area (Fig. 6), confirming that this down-regulation of leaf photosynthesis may be attributed to the decline of stomatal conductance through reducing stomatal openness when soybean plants exposed to high CO_2 concentrations. Additionally, the less regular stomatal distribution pattern on the adaxial leaf surface of soybean plants as evidenced by the larger Lhat (d) at higher CO_2 concentrations may contribute to the decline of stomatal conductance through increasing the average distance of CO_2 diffusion from stomata to chloroplasts [47, 63]. Overall, the fewer stomata and smaller stomatal pore aperture, as well as the more irregular spatial distribution patterns at high CO_2 concentrations may partially explain the decline of stomatal conductance in the current study. Also, several recent studies have claimed that down-regulation of leaf photosynthesis is well associated with the declined stomatal conductance, which is mainly attributed to decreases of stomatal density and stomatal openness [21, 70, 71]. It should be noted that the declined G_s does not necessarily reduce leaf photosynthesis when plants exposed to elevated CO_2 concentrations [24]. Nevertheless, the leaf photosynthesis-G_s relationship did follow a linear equation in the current study ($R^2 = 0.81$), indicating that the decreased stomatal conductance under high CO_2 concentrations contributed to leaf photosynthesis down-regulation of soybean plants.

Down-regulation of leaf photosynthesis associates with anatomical structure of mesophyll tissues

In addition to stomatal traits, the down-regulation of leaf photosynthesis is also associated with changes in the anatomical structure of mesophyll tissues at the high CO_2 concentration [72–74]. Our results showed that the cell area of palisade and spongy tissues were increased by 15 and 28% as CO_2 concentration increased from 400 ppm to 600 ppm, while the cell area of both the palisade and spongy tissues were marginally declined with further increase of CO_2 concentration (Table 3). This decreased cell area of mesophyll tissues is likely to explain the down-regulation of leaf photosynthesis, because the smaller mesophyll cells at higher CO_2 concentration may lead to narrow space for accommodating fewer chloroplasts through constraining the cell expansion, and thus limit the carbon gain efficiency of plants [52–54]. Xu also found that the average cell area of mesophyll tissue was decreased by about 30% at higher CO_2 concentration [60]. Interestingly, we also found linearly positive relationships between leaf photosynthesis and mesophyll cell area, confirming that the down-regulation of leaf photosynthesis may be partially due to the smaller total mesophyll size (palisade and spongy tissues) of soybean plants under high CO_2 environments.

Changes in leaf non-structural carbohydrates and nitrogen attribute to down-regulation of photosynthesis

It is well documented that the down-regulation of photosynthesis is usually associated with changes in leaf chemical composition such as the N availability deficit [32–34], the lower Rubisco concentration and activity [33, 34] as well as the source-sink imbalance due to carbohydrates accumulation in leaves under high CO_2 concentration [29, 36–38]. Previous studies have demonstrated that elevated CO_2 concentration enhances leaf C/N ratio mainly due to the decline of N concentration through a process known as “N dilution” [61]. Our results showed that the leaf N was significantly decreased with increasing CO_2 concentration from 400 ppm to 1200 ppm (Table 4), which may also attribute to the down-regulation of leaf photosynthesis, because leaf N is closely related to photosynthetic enzymes such as Rubisco [17]. However, several previous studies have claimed that the Rubisco concentration and activity of plants were substantially reduced at high CO_2 concentration, because leaf N was prior to enzymes relating to

the metabolic processes of carbohydrates than invested to Rubisco when plants were exposed to high CO_2 environments [75]. Furthermore, it is important to note that hexokinase is a key functional enzyme for mediating sugar sensing, and thus may contribute the down-regulation of photosynthesis through decreasing the Rubisco concentration with inhibiting the expression of photosynthetic genes [38, 62].

In addition to leaf N, the down-regulation of photosynthesis induced by elevated CO_2 is also possibly attributed to the accumulation of carbohydrates in leaves when plants subjected to high CO_2 environments for a long time period [29, 46, 63, 64]. Our results showed that the total non-structural carbohydrates in leaves (TNC) was dramatically declined at higher CO_2 concentrations (Table 5), suggesting that the source-sink imbalance of carbohydrates should not be a limiting factor for the down-regulation of photosynthesis in the current study. Moreover, we also found a positive linear relationship between leaf photosynthesis and TNC (Fig. 8), which directly supported the above conclusion that the imbalance of carbohydrate concentration in the source and sink contributed little to the leaf photosynthesis down-regulation of soybean plants subjected to high CO_2 concentrations.

Conclusions

We found that the net photosynthesis rate of soybean was dramatically declined with elevated CO_2 concentration from 400 ppm to 1600 ppm following a typical quadratic relationship. This down-regulation of leaf photosynthesis at higher CO_2 concentrations can be attributed to the limiting effects on stomatal diffusion processes and nitrogen availability as well as the changes in the biochemical and photochemical efficiency of photosynthesis. Overall, our results suggest that the continuously increasing CO_2 concentration in the future may lead to negative impacts on agricultural production through hurting crop growth and/or reducing crop yield. Nevertheless, most of the projections estimated the plant growth and crop production according to the earlier results from "doubling-CO_2 experiments" with strong CO_2 fertilization effect. Therefore, many current climate change models may underestimate the potential risk of climate change on agricultural production mainly due to the overestimated strong CO_2 fertilization effect on plant growth and crop yield under future elevated atmospheric CO_2 concentration and climate change.

Methods

Growth chamber experiments

We bought soybean seeds from the Wotu seed company in Hebei Province of China. We grew three plants in each pot (30 cm diameter × 50 cm long), then set up five pots in each of the seven walk-in environmental growth chambers for 90 days CO_2 treatment, where the CO_2 concentration was regulated to ambient concentration (400 ppm) or elevated concentrations (600, 800, 1000, 1200, 1400 and 1600 ppm). The ambient and elevated CO_2 concentrations within the chambers were maintained through a CO_2 tank containing high purity CO_2 gas (99.99%) to avoid any hurt or pollution on winter wheat plants. All of the seven growth chambers were maintained with the same other environmental factors including relative humidity of 65%, photosynthetic photon flux density (PPFD) of 1000 μmol m^{-2} s^{-1}, temperature of 25/21 °C (day/night), and 12-h photoperiod for the 90 days treatment. These winter wheat plants were fertilized with half-strength Hoagland's solution twice weekly (150 mL per pot) and irrigated once daily with plain tap water (200 mL per pot) during the establishment and treatment periods of soybean plants under elevated CO_2 concentrations.

Measuring leaf gas exchange

We performed the measurements of leaf gas exchange at the end of the CO_2 treatment period. We randomly selected one fully expanded leaf from each pot for leaf gas exchange measurement ($n = 5$) with a portable photosynthesis system (LI-6400XT; LICOR, Inc.). These selected leaves were firstly equilibrated at the corresponding growth CO_2 levels with saturating PPFD of 1500 μmol photon m^{-2} s^{-1} and growth temperature of 25 °C. The portable photosynthesis system automatically controlled the CO_2 concentrations in the cuvette using an injector system combined with a CO_2 mixer. All of the measurements on leaf gas exchange were performed with the vapor pressure deficit (*VPD*) lower than 1.5 kPa to avoid moisture limitation. Then, the photosynthesis vs intercellular CO_2 (A_n-C_i) curves were measured at cuvette chamber CO_2 of 50, 100, 150, 200, 300, 400, 600, 800, 1000, 1200, 1400, and 1600 ppm. Data from A_n-C_i curves were used to compare treatment effects on the light-saturated net photosynthetic rates (A_n) at ambient or elevated CO_2 of their growing condition. A_n estimation method was used to obtain the maximum carboxylation rate of Rubisco (V_{cmax}), and the maximum capacity of electron transport mediated ribulose bisphosphate (RuBP) regeneration (J_{max}) for each observed A_n-C_i curve. Meanwhile, stomatal conductance (G_s), intercellular CO_2 concentration (C_i), transpiration rate (T_r), and dark respiration rate (R_d) were also determined with the portable photosynthesis system (LI-6400XT; LICOR, Inc.). In addition, the leaf-level water use efficiency (*WUE*) was determined by the values of the net photosynthetic rate (A_n) and transpiration rate (T_r) according to the formula $WUE = A_n / T_r$.

Measuring morphological traits of individual stoma and spatial distribution pattern of stomata

We randomly selected five fully expanded ear leaves at the heading stage in each of the ambient and elevated CO_2

concentration plots to determine the stomatal characteristics. We sampled impressions of stomata with colorless nail polish from the middle section of the adaxial and abaxial leaf surfaces. Firstly, the adaxial and abaxial leaf epidermis were carefully cleaned with degreased cotton balls and then smeared with nail varnish from the mid-area between the leaf edge and the central vein for half an hour. The thin film with stomatal impression (approximately 5 mm × 15 mm) was peeled off from the leaf surface and mounted on a glass slide, and immediately covered with a cover slip and lightly pressured with a fine-point tweezer [47, 63]. We photographed the stomatal features with a microscope (DM2500, Leica Corp, Germany) equipped with a digital camera (DFC 300-FX, Leica Corp, Germany), and then analyzed thirty separate fields of 0.16 mm in each leaf section. We also combined and counted the stomata on each surface for calculating stomatal density (SD) of the adaxial and abaxial surface, respectively [47]. Moreover, we randomly selected six digital photographs of the adaxial and abaxial surfaces to measure the stomatal length (SL), stomatal width (SW), stomatal area (SA) and stomatal perimeter (SP) using AutoCAD 2010 software. In addition, we calculated stomatal shape index (SSI), which is calculated by the function that shape index= $\frac{\sqrt{SA}}{SP} \times 100\%$, where SA is the stomatal area and SP is the stomatal perimeter. The stomatal area index (SAI) is defined as the total stomatal area per unit leaf area calculating as stomatal average density × stomatal area per stoma × 100%. In addition to stomatal density and pore traits, we also characterized the spatial distribution pattern of stomata for each image by digitizing the stomatal positions into a shape file in GIS with the ArcMap software [47]. The spatial distribution pattern of stomata on leaves was quantified using the Ripley's K-function with generating the x and y coordinates of stomata for each image in GIS and then calculating the Lhat (d) value (the transformed K value) based on these stomatal coordinates using the R statistic software. We compared the Lhat (d) values at different scales (distances) for detecting the spatial distribution pattern of stomata with the upper and lower boundaries generated by the 95% confidence level with the Monte Carlo simulations of 100 replicates [47, 76]. In the current study, we only reported the spatial distribution patterns of stomata on the middle section of the leaves due to the large number of stomatal images of winter wheat leaves.

We snapped three leaf pieces (2 mm × 2 mm) from the middle section of each leaf and fixed them with 2.5% (v/v) glutaraldehyde (0.1 M phosphate buffer, pH 7.0) to visualize the changes in stomatal morphology among different CO_2 concentrations. Firstly, we washed these leaf samples several times with buffer and fixed them in 1% (v/v) osmium tetroxide for three hours and these samples were dehydrated with an ethanol series. Then, these leaf samples were carefully coated with gold in a high-vacuum evaporation unit. Finally, we examined and photographed the morphological traits of stomata with a scanning electron microscopy (FEI Corp, USA).

Measuring leaf anatomical structures

Changes in the leaf internal anatomy of the winter wheat plants exposed to different CO_2 concentrations were examined with leaf cross-sections under a light microscopy [77]. These images of leaf cross-sections were collected from the middle section of leaves to observe and measure leaf anatomical features using Image J software (NIH, USA). We estimated leaf mesophyll thickness between epidermal layers at five points in each cross-section [78]. We also randomly selected 20 clear palisade layer cells and 20 sponge layer cells from each leaf cross-section image to measure cell length, cell width, cell area, and cell perimeter with an Auto CAD software.

Analyzing leaf non-structural carbohydrates and nitrogen

We collected leaf samples from each pot as a replicate ($n = 5$ pots) for analyzing the non-structural carbohydrates. These sampled leaves were dried with an oven at 75 °C for 48 h to consistent weight, and then these samples were ground to fine powder for spectrophotometrically analyzing glucose, fructose, sucrose, and starch with a glucose kit [79]. Similarly, we also sampled plant tissues from each pot (n = 5 pots) for analyzing the total carbon (C) and nitrogen (N) in different plant tissues (leaf, stem, and root) with an elemental analyzer [80]. All of the analyses were expressed on a percentage dry matter basis.

Analyzing data

We used the one-way ANOVA to analyze the effects of CO_2 on the stomatal traits, soluble sugar and starch concentrations, carbon and nitrogen contents, as well as morphological and anatomical features. Two-way ANOVA was employed to test the effects of CO_2 concentration and leaf surface position (abaxial vs. adaxial) on the morphological traits of stomata with statistically significant differences at $p < 0.05$ level. We also employed linear and non-linear regressions for estimating the relationships between CO_2 concentration and other variables. The raw data from the leaf photosynthesis measurements were processed in Excel spreadsheets where the non-linear A_n-C_i curve fitting was performed [81]. The net assimilation rate (A_n) versus intercellular CO_2 concentration (A_n-C_i curve), was fitted to estimate the maximum carboxylation rate (V_{cmax}), maximum electron transport rate (J_{max}) based on the measurements of A_n-C_i curves. In addition, linear and non-linear (quadratic equations) regressions were employed to examine the relationships between CO_2 concentration and other variables.

Abbreviations

A_n: Net assimilation rate; A_n-C_i curve: Net assimilation rate versus intercellular CO_2 concentration curve; C_i: intercellular CO_2 concentration; G_s: stomatal conductance; J_{max}: Maximum electron transport rate; R_d: dark respiration rate; V_{cmax}: Maximum carboxylation rate; *VPD*: vapor pressure deficit

Acknowledgments

We gratefully thank the anonymous reviewer for the constructive comments and suggestions on revising the manuscript. We also acknowledge Mr. Steven Xu (Rutgers University, USA) for editing the English of the manuscript.

Funding

This research was partially supported by the Natural Science Foundation of China (31400418), Natural Science Foundation of Hebei Province (C2016402088), Young Outstanding Innovative Talents of Hebei Province (BJ2016012), and the China Postdoctoral Science Foundation funded project (2014 M561044 and 2016 T90128). The funders have no role in the study design, data analysis and interpretation, and manuscript writing, but just provide the financial support.

Availability of data and materials

The datasets used and/or analyzed during the current study are available from the corresponding author on reasonable request.

Authors' contributions

YZ, MX, LH, XZ and FL designed the experiments. LH, JY, LG, HZ, CM, and XZ performed the experiments and analyzed the data. FL, JY, YZ, HZ, XZ, CM, MX and analyzed the data and wrote the manuscript. All authors read and approved the final manuscript.

Ethics approval and consent to participate

Not applicable.

Consent for publication

Not applicable.

Competing interests

The authors declare that they have no competing interests.

Publisher's Note

Author details

[1]School of Water Conservancy and Hydropower, Hebei University of Engineering, Handan 056038, China. [2]School of Agro-Grassland Science, Nanjing Agricultural University, Nanjing 210095, People's Republic of China. [3]Department of Biology, University of Pennsylvania, Philadelphia, PA 19104, USA. [4]Key Laboratory of Geospatial Technology for the Middle and Lower Yellow River Regions, College of Environment and Planning, Henan University, Kaifeng 475004, China. [5]Center for Remote Sensing and Spatial Analysis, Department of Ecology, Evolution and Natural Resources, Rutgers University, 14 College Farm Road, New Brunswick, NJ 08901, USA.

Received: 12 January 2019 Accepted: 18 April 2019
Published online: 13 June 2019

References

1. Gunderson CA, Wullschleger SD. Photosynthetic acclimation in trees to rising CO_2: a broader perspective. Photosynth Res. 1994;39:369–88.
2. Aljazairi S, Nogues S. The effects of depleted, current and elevated growth CO_2 in wheat are modulated by water availability. Environ Exp Bot. 2015; 112:55–66.
3. Jahnke S. Atmospheric CO_2 concentration does not directly affect leaf respiration in bean or polar. Plant Cell Environ. 2001;24:1139–51.
4. Erice G, Irigoyen JJ, Perez P, Martínez-Carrasco R, Sánchez-Díaz M. Effect of elevated CO_2, temperature and drought on photosynthesis of *nodulated alfalfa* during a cutting regrowth cycle. Physiol Plant. 2006;126:458–68.
5. Hamilton IIIEW, Heckathorn SA, Joshi P, Wang D. Barua D. Interactive effects of elevated CO_2 and growth temperature on the tolerance of photosynthesis to acute heat stress in C_3 and C_4 species. J Integr Plant Biol 2008;50:1375–1387.
6. IPCC. Summary for policy makers: climate change 2013: the physical science basis. In: Church J, Clark P, Cazenave A, Gregory J, Jevrejeva S, Levermann A, Merrifield M, Milne G, Nerem SR, Nunn P, Payne A, Pfeffer WT, Stammer D, Alakkat U, editors. Contribution of working group I to the fifth assessment report of the intergovernmental panel on climate change. UK: Cambridge University Press; 2013.
7. NASA: Global climate change: Vital signs of the planet 2014. Available at: http:// climate. nasa.
8. Wand SJE, Midgley GF, Jones MH. Responses of wild C_4 and C_3 grass (*Poaceae*) species to elevated atmospheric CO_2 concentration: a meta-analytic test of current theories and perceptions. Glob Change Biol. 1999;5: 723–41.
9. Medlyn BE, Barton CVM, Broadmeadow MSJ, Ceulemans R, De Angelis P, Forstreuter M, et al. Stomatal conductance of forest species after long-term exposure to elevated CO_2 concentration: a synthesis. New Phytol. 2000;149: 247–64.
10. Suter D, Frehner M, Fischer BU. Elevated CO_2 increases carbon allocation to the roots of *Lolium perenne* under free-air CO_2 enhancement but not in a controlled environment. New Phytol. 2002;154:65–75.
11. Gonzàlez-Meler MA, Blanc-Betes E, Flower CE. Plastic and adaptive responses of plant respiration to changes in atmospheric CO_2 concentration. Physiol Plant. 2009;37:473–84.
12. Zhang L, Wu D, Shi H. Effects of elevated CO_2 and N addition on growth and N_2 fixation of a Legume subshrub (*Caragana microphylla* Lam.) in temperate grassland in China. PLoS ONE. 2011;6:e26842.
13. Drake BG, González-Meler MA, Long SP. More efficient plants: a consequence of rising atmospheric CO_2. Annu Rev Plant Physiol Plant Mol Biol. 1997;48:609–39.
14. Lee TD, Tjoelker MG, Ellsworth DS. Leaf gas exchange responses of 13 prairie grassland species to elevated CO_2 and increased nitrogen supply. New Phytol. 2001;150:405–18.
15. Ainsworth EA, Davey PA, Bernacchi CJ, Dermody OC, Heaton EA, Moore DJ, et al. A meta-analysis of elevated [CO_2] effects on soybean (*Glycine max*) physiology, growth and yield. Glob Chang Biol. 2002;8:695–709.
16. Curtis PS, Wang X. A meta-analysis of elevated CO_2 effects on woody plant mass, form, and physiology. Oecologia. 1998;113:299–13.
17. Ziska LH, Bunce JA. Sensitivity of field-grown soybean to future atmospheric CO_2: selection for improved productivity in the 21st century. Aust J Plant Physiol. 2000;27:979–84.
18. Poorter H, Navas M. Plant growth and competition at elevated CO_2: on winners, losers and functional groups. New Phytol. 2003;157:175–98.
19. Morgan JA, Milchunas DG, LeCain DR. Carbon dioxide enhancement alters plant community structure and accelerates shrub growth in the short grass steppe. Proc Natl Acad Sci U S A. 2007;104:14724–9.
20. Yu J, Chen L, Xu M. Effects of elevated CO_2 on physiological responses of tall fescue to elevated temperature, drought stress, and the combined stress. Crop Sci. 2012;52:1848–58.
21. Singh SK, Reddy VR. Methods of mesophyll conductance estimation: its impact on key biochemical parameters and photosynthetic limitations in phosphorus stressed soybean across CO_2. Physiol Plant. 2016;157: 234–54.
22. Farquhar GD, Von Caemmerer S, Berry JA. A biochemical model of photosynthetic CO_2 fixation in C_3 species. Planta. 1980;149:178–90.
23. Long SP. Modification of the response of photosynthetic productivity rising temperature by atmospheric CO_2 concentration-has its importance been underestimated. Plant Cell Environ. 1991;14:729–39.
24. Long SP, Ainsworth EA, Rogers A. Rising atmospheric carbon dioxide: plants FACE the future. Ann Rev Plant Biol. 2004;55:591–628.
25. Duarte B, Santos D, Marques JC, Caçador I. Ecophysiological adaptations of two halophytes to salt stress: photosynthesis, PS II photochemistry and anti-oxidant feedback-implications for resilience in climate change. Plant Physiol Biochem. 2013;67:178–88.
26. Salvucci ME, Crafts-Brandner SJ. Inhibition of photosynthesis by heats tress: the activation state of rubisco as a limiting factor in photosynthesis. Physiol Plant. 2004;120:179–86.
27. Casteel CL, O'Neill BF, Zavala JA, Bilgin DD, Berenbaum MR, Delucia EH. Transcriptional profiling reveals elevated CO_2 and elevated O_3 alter resistance of soybean (*Glycine max*) to Japanese beetles (*Popillia japonica*). Plant Cell Environ. 2008;31:419–34.

28. Robredo A, Perez-Lopez U, Lacuesta M, Mena-Petite A, Munoz-Rueda A. Influence of water stress on photosynthetic characteristics in barley plants under ambient and elevated CO_2 concentrations. Biol Plant. 2010;54:285–92.
29. Kanemoto K, Yamashita Y, Ozawa T, Imanishi N, Nguyen NT, Suwa R, et al. Photosynthetic acclimation to elevated CO_2 is dependent on N partitioning and transpiration in soybean. Plant Sci. 2009;177:398–403.
30. Cotrufo MF, Ineson P, Scott A. Elevated CO_2 reduces then nitrogen concentration of plant tissues. Glob Chang Biol. 1998;4:43–54.
31. Lindroth RL, Roth S, Nord heim EV. Genotypic variation in response of quaking aspen (*Populus tremuloides*) to atmospheric CO_2 enrichment. Oecologia, 2001;126:371–379.
32. Jifon J, Wolfe D. Photosynthetic acclimation to elevated CO_2 in *Phaseolus vulgaris* L. is altered by growth response to nitrogen supply. Glob Chang Biol. 2002;8:1019–27.
33. Eichelmann H, Talts E, Oja V, Padu E, Laisk A. Rubisco in planta kcat is regulated in balance with photosynthetic electron transport. J Exp Bot. 2009;60:4077–88.
34. Sanz-Sáez Á, Erice G, Aranjuelo I, Aroca R, Ruíz-Lozano JM, Aguirreolea J, et al. Photosynthetic and molecular markers of CO_2 mediated photosynthetic down regulation in nodulatedalf alfa. J Integ Plant Biol. 2013;55:721–34.
35. Ziska LH, Bunce JA, Caulfield FA. Rising atmospheric carbon dioxide and seed yield of soybean genotypes. Crop Sci. 2001;41:385–91.
36. Davey PA, Olcer H, Zakhleniuk O, Bernacchi CJ, Calfapietra C, Long SP, et al. Can fast-growing plantation tree escape biochemical down-regulation of photosynthesis when grown throughout their complete production cycle in the open air under elevated carbon dioxide? Plant Cell Environ. 2006;29: 1235–44.
37. Atkin O, Millar HA, Turnbull MH. Plant respiration in a changing world. New Phytol. 2010;187:268–72.
38. Atkin O. New Phytologist and the 'fate' of carbon in terrestrial ecosystems. New Phytol. 2015;205:1–3.
39. Wheeler RM, Mackowiak CL, Siegriest LM, Sager JC. Supraoptimal carbon dioxide effects on growth of soybean (*Glycine max* (L.) Merr.). J Plant Physiol. 1993;142:173–8.
40. Crous KY, Zaragoz-Castells J, Löw M. Seasonal acclimation of leaf respiration in *Eucalyptus saligna* trees: impacts of elevated atmospheric CO_2 and summer drought. Glob Chang Biol. 2011;17:1560–76.
41. Lichtenthaler HK. The1-deoxy-D-xylulose-5-phosphate pathway of is oprenoid biosynthesis in plants. Annu Rev Plant Physiol Plant Mol Biol. 1999; 50:47–65.
42. Hamilton JG, Thomas RB, Delucia EH. Direct and indirect effects of elevated CO_2 on leaf respiration in a forest ecosystem. Plant Cell Environ. 2001;24: 975–82.
43. Gu LH, Pallardy SG, Tu K, Law BE, Wullschleger S. Reliable estimation of biochemical parameters from C_3 leaf photosynthesis-intercellular carbon dioxide response curves. Plant Cell Environ. 2010;33:1852–74.
44. Kane K, Dahal KP, Badawi MA, Houde M, Hüner NP, Sarhan F. Long-term growth under elevated CO_2 suppresses biotics tress genes in non-acclimated, but not cold-acclimated winter wheat. Plant Cell Physiol. 2013; 54:1751–68.
45. Wang L, Feng ZZ, Schjoerring JK. Effects of elevated atmospheric CO_2 on physiology and yield of wheat (*Triticum aestivum* L.): a meta-analytic test of current hypotheses. Agric Ecosyst Environ. 2013;178:57–63.
46. Liu J, Zhang J, He C, Duan A. Genes responsive to elevated CO_2 concentrations in triploid white poplar and integrated gene network analysis. PLoS One. 2014;9:e98300.
47. Xu M. The optimal atmospheric CO_2 concentration for the growth of winter wheat (*Triticum aestivum*). J Plant Physiol. 2015;184:89–97.
48. Logan BA, Hricko CR, Lewis JD, Ghannoum O, Phillips NG, Smith R, Conroy JP, Tissue DT. Examination of pre-industrial and future CO_2 reveals the temperature-dependent CO_2 sensitivity of light energy partitioning at PSII in eucalypts. Funct Plant Biol. 2010;37:1041–9.
49. Tissue DT, Lewis JD. Photosynthetic responses of cottonwood seedlings grown in glacial through future atmospheric CO_2 vary with phosphorus supply. Tree Physiol. 2010;30:1361–72.
50. Ayub G, Smith RA, Tissue DT, Atkin OK. Impacts of drought on leaf respiration in darkness and light in *Eucalyptus saligna* exposed to industrial-age atmospheric CO_2 and growth temperature. New Phytol. 2011;190:1003–18.
51. Pritchard SG, Peterson CM, Prior SA, Rogers HH. Elevated atmospheric CO_2 differentially affects needle chloroplast ultrastructure and phloem anatomy in *Pinus palustris*: interactions with soil resource availability. Plant Cell Environ. 1997;20:461–71.
52. Loveys BR, Atkinson LJ, Sherlock DJ, Roberts RL, Fitter AH, Atkin OK. Thermal acclimation of leaf and root respiration: an investigation comparing inherently fast-and slow-growing plant species. Glob Chang Biol. 2003;9: 895–910.
53. Marchi S, Tognetti R, Minnocci A, Borghi M, Sebastiani L. Variation in mesophyll anatomy and photosynthetic capacity during leaf development in a deciduous mesophyte fruit tree (*Prunus persica*) and an evergreen sclerophyllous Mediterranean shrub (*Olea europaea*). Trees-Structure Funct. 2008;22:559–71.
54. Jin B, Wang L, Wang J, Jiang K, Wang Y, Jiang X, et al. The effect of artificial warming on leaf functional traits, leaf structure and leaf biochemistry in Arabidopsis thaliana. BMC Plant Biol. 2011;11:35.
55. Taylor G, Ranasinghe S, Bosac C, Gardner SDL, Ferris R. Elevated CO_2 and plant growth-cellular mechanism and responses of whole plants. J Exp Bot. 1994;45:1761–74.
56. Ranasinghe S, Taylor G. Mechanism for increased leaf growth in elevated CO_2. J Exp Bot. 1996;47:349–58.
57. Ferris R, Sabatti M, Miglietta F, Mills RF, Taylor G. Leaf area is stimulated in *Populus* by free air CO_2 enrichment (POPFACE), through increased cell expansion and production. Plant Cell Environ. 2001;24:305–15.
58. Griffin KL, Anderson OR, Gastrich MD, Lewis JD, Lin GH, Schuster W, et al. Plant growth in elevated CO_2 alters mitochondrial number and chloroplast fine structure. Proc Natl Acad Sci U S A. 2001;98:2473–8.
59. Gorsuch PA, Pandey S, Atkin OK. Temporal heterogeneity of cold acclimation phenotypes in Arabidopsis leaves. Plant Cell Environ. 2010;33: 244–58.
60. Xu CY, Salih A, Ghannoum O, David T. Tissue. Leaf structural characteristics are less important than leaf chemical properties in determining the response of leaf mass per area and photosynthesis of *Eucalyptus saligna* to industrial-age changes in $[CO_2]$ and temperature. J Exp Bot. 2012;63:5829–41.
61. Luo GM, Lai XL, Jiang HS, Zhang KX. Size variation of the end Permian conodont *Neogondolella* at Meishan section, Changxing, Zhejiang and its significance. SCI CHINA SER D. 2006;49:337–47.
62. Kelly G, Sade N, Attia Z, Secchi F, Zwieniecki M, Holbrook NM, Asher L, Alchanatis V, Moshelion M, Granot D. Relationship between hexokinase and the aquaporin PIP1 in the regulation of photosynthesis and plant growth. PLoS ONE. 9(2):e87888. https://doi.org/10.1371/journal.pone.0087888.
63. Zheng YP, Li F, Hao LH, Shedayi AA, Guo LL, Ma C, Huang BR, Xu M. The optimal CO_2 concentrations for the growth of three perennial grass species. BMC Plant Biol. 2018;18:27.
64. Hogy P, Brunnbauer M, Koehler P, Schwadorf K, Breuer J, Franzaring J, et al. Grain quality characteristics of spring wheat (*Triticum aestivum*) as affected by free-air CO_2 enrichment. Environ Exp Bot. 2013;88:11–8.
65. Rawson HM. Yield responses of two wheat genotypes to carbon dioxide and temperature in field studies using temperature gradient tunnels. Aust J Plant Physiol. 1995;22:23–32.
66. Pleijel H, Gelang J, Sild E, Danielsson H, Younis S, Karlsson PE, et al. Effects of elevated carbon dioxide, ozone and water availability on spring wheat growth and yield. Physiol Plant. 2000;108:61–70.
67. Vu JCV, Allen LH Jr, Boote KJ, Bowes G. Effects of elevated CO_2 and temperature on photosynthesis and rubisco in rice and soybean. Plant Cell Environ. 1997;20:68–76.
68. BassiriRad H, Gutschick VP, Lussenhop J. Root system adjustments: regulation of plant nutrient uptake and growth responses to elevated CO_2. Oecologia. 2001;126:305–20.
69. Patrick B, Bingru H. Growth and physiological responses of creeping bentgrass (*Agrostis stolonifera*) to elevated carbon dioxide concentrations. Hortic Res. 2014;1:14021.
70. Bernacchi CJ, Morgan PB, Ort DR, Long SP. The growth of soybean under free air $[CO_2]$ enrichment (FACE) stimulates photosynthesis while decreasing in vivo rubisco capacity. Planta. 2005;220:434–46.
71. Singh SK, Badgujar GB, Reddy VR, Fleisher DH, Timlin D. Carbon dioxide diffusion across stomata and mesophyll and photo-biochemical processes as affected by growth CO_2 and phosphorus nutrition in cotton. J Plant Physiol. 2013;170:801–13.
72. Uprety DC, Dwivedi N, Mohan R, Paswan G. Effect of elevated CO_2 concentration on leaf structure of *Brassica juncea* under water stress. Biol Plant. 2001;44:149–52.

73. Wang XZ, Anderson OR, Griffin KL. Chloroplast numbers, mitochondrion numbers and carbon assimilation physiology of *Nicotiana sylvestris* as affected by CO_2 concentration. Environ Exp Bot. 2004;51:21–31.
74. Lewis JD, Ward JK, Tissue DT. Phosphorus supply drives nonlinear responses of cottonwood (*Populus deltoides*) to increases in CO_2 concentration from glacial to future concentrations. New Phytol. 2010;187:438–48.
75. Ziska LH, Bunce JA. Growth and photosynthetic response of three soybean cultivars to simultaneous increases in growth temperature and CO_2. Physiol Plant. 1995;94:575–84.
76. Ripley BD. Spatial statistics in R. R News. 2001;1:14–5.
77. Sage TL, Williams EG. Structure, ultrastructure, and histochemistry of the pollen tube pathway in the milkweed *Asclepias exaltata* L. Sex Plant Reprod. 1995;8:257–65.
78. Pengelly JJL, Sirault XRR, Tazoe Y, Evans JR, Furbank RT, Caemmerer S. Growth of the C_4 dicot *Flaveria bidentis*: photosynthetic acclimation to low light through shifts in leaf anatomy and biochemistry. J Exp Bot. 2010;61:4109–22.
79. Hendrix DL. Rapid extraction and analysis of nonstructural carbohydrates in plant tissues. Crop Sci. 1993;33:1306–11.
80. Way DA, Sage RF. Elevated growth temperatures reduce the carbon gain of black spruce [*Picea mariana* (mill.) B. S. P.]. Glob Chang Biol. 2008;14:624–36.
81. Sharkey TD, Bernacchi CJ, Farquhar GD, Singsaas EL. Fitting photosynthetic carbon dioxide response curves for C_3 leaves. Plant Cell Environ. 2007;30:1035–40.